Ionoluminescence induced by swift heavy ions in silica and quartz: A comparative analysis

D. Jimenez-Rey O. Peña-Rodríguez J. Manzano-Santamaría J. Olivares A. Muñoz-Martin
A. Rivera F. Agulló-López

A B S T R A C T

Ionoluminescence (IL) of the two SiO_2 phases, amorphous silica and crystalline quartz, has been comparatively investigated in this work, in order to learn about the structural defects generated by means of ion irradiation and the role of crystalline order on the damage processes. Irradiations have been performed with Cl at 10 MeV and Br at 15 MeV, corresponding to the electronic stopping regime (i.e., where the electronic stopping power S_e is dominant) and well above the amorphization threshold. The light-emission kinetics for the two main emission bands, located at 1.9 eV (652 nm) and 2.7 eV (459 nm), has been measured under the same ion irradiation conditions as a function of fluence for both, silica and quartz. The role of electronic stopping power has been also investigated and discussed within current views for electronic damage. Our experiments provide a rich phenomenological background that should help to elucidate the mechanisms responsible for light emission and defect creation.

1. Introduction

Silicon dioxide (SiO_2), either crystalline (quartz) or amorphous (silica), is a relevant compound very abundant in nature that presents many applications, as functional and structural materials, in a large variety of fields ranging from photonics and microelectronics to geology (dating) and archaeology. In several of these technologies, both materials are subjected to high fluxes of radiation such as photons in laser technology, or neutrons and charged particles in accelerators and nuclear fission and fusion facilities [1,2]. Therefore, a lot of research activity has been devoted to understand the effects of irradiation on the atomic and electronic structures of the crystalline and amorphous phase of SiO_2. Interest in the damage produced by high energy heavy mass (swift) ions has strongly increased recently because electronic mechanisms may dominate on elastic nuclear collisions and the induced damage presents a considerable number of differential features not yet sufficiently understood [3–6].

Likewise, luminescence [7,8] is a very sensitive technique, often applied for characterization of dielectric and semiconductor materials. It provides information on the electronic structure of the solid, particularly on intra-gap levels associated to impurity and defect centers, such as those introduced by irradiation. In particular, the luminescence induced by ion-beam irradiation, commonly named ionoluminescence (IL), is an appropriate technique to investigate the microscopic processes accompanying the generation of damage, its kinetic evolution with the irradiation fluence, and the formation of color centers [9–14]. IL can be considered as an Ion Beam Analysis (IBA) technique that is complementary to Rutherford backscattering spectrometry (RBS), particle-induced X-ray emission (PIXE), and nuclear reaction analysis (NRA) methods. However, IL is far less used that the other IBA techniques because the analysis of the IL data is more complex and requires theoretical methods not yet sufficiently developed.

The purpose of this work focuses on a comparative study of the ionoluminescence induced on crystalline quartz and amorphous silica by irradiation with Cl at 10 MeV and Br at 15 MeV; i.e., in the electronic stopping regime. It is well known [4,5] that every swift ion impact generates a nanometric amorphous track, whenever the electronic stopping power is above a certain critical threshold value, estimated around 2 keV/nm. Moreover, the electronic damage is cumulative so that, even below threshold, amorphization can be still achieved through track overlapping [15]. The IL spectra and yields will be discussed within such scheme, so that new relevant information could be obtained on

track formation and crystal amorphization. In particular, it will be shown that IL is strongly related to the number of stressed bonds, suggesting its possible use as a sensor of structural disorder.

2. Experimental

The high-purity synthetic quartz and silica samples used in this work were provided by Crystran and EMS, respectively. In both cases the OH content is below 10 ppm and the total impurity content below 30 ppm. The original wafers of 10 cm diameter (1 mm thickness) were cut into pieces of 10×10 mm^2 and covered by a copper mask to define an irradiation area of 6×6 mm^2 and avoid electric arcs. Samples were irradiated in a standard scattering chamber, at a vacuum of 10^{-4} Pa, connected to a 5 MV tandem accelerator in the Centro de Micro-Análisis de Materiales (CMAM) [16]. Irradiations were performed with Cl at 10 MeV and Br at 15 MeV, using currents in the range 10–15 nA to avoid overheating of the samples. Fluences were determined by direct current integration from the target (sample holder) using electron suppression. The electronic stopping powers (S_e) at the sample surface for the ions and materials used in this work are shown in Table 1.

Fig. 1 shows a schematic diagram of the experimental setup used to measure the IL spectra. The IL emission was transmitted through a silica window port placed at 45° with respect to the ion beam and collected and focused with a 25-mm-diameter, 4-cm-focal-length silica lens into a silica optical fiber of 1 mm diameter, located outside of the vacuum chamber. The light was guided to a compact spectrometer, QE6500 (Ocean Optics Inc.), configured with a multichannel array detector for measuring simultaneously the whole spectrum in the range 200–850 nm with a spectral resolution better than 2 nm. The IL spectra were recorded using an integration time of 5 s. In the presented graphs we have converted the IL yield (originally in units of $I(\lambda)\mathrm{d}\lambda$) to $I(E)\mathrm{d}E$ by multiplying the measured counts by λ^2; this is required because the original units distort the view obtained in the energy plots [17]. Due to the high sensitivity of the IL against small current fluctuations (around 1 nA), it was necessary to record the real-time evolution of the current in order to discriminate variations in the IL produced by the kinetics of damage evolution from those associated with current changes. It should be recalled that the dependence of IL with the ion flow is not necessarily linear for large variations of the latter; therefore, this correction is only valid for small current fluctuations.

3. Results

Fig. 2 shows some representative IL spectra of silica (Fig. 2a and c) and quartz (Fig. 2b and d) irradiated with Br at 15 MeV and common fluences of 2.5×10^{12} cm^{-2} (Fig. 2a and b) and 3×10^{13} cm^{-2} (Fig. 2c and d). These two fluences, respectively, correspond to low and high fluences in the scale of our experiments. The observed color of the irradiated samples changes with material and fluence as illustrated in the corresponding inset photos accompanying the spectra. The spectra have been in all cases decomposed into four different emission bands, whose peak positions and widths are listed in Table 2. All of these bands have been previously reported in the literature and ascribed to substitutional impurities

Table 1
Electronic stopping powers for the ions and materials used in this work, calculated using SRIM 2008 [35,36].

	Cl at 10 MeV	Br at 15 MeV
Silica	3.6 keV/nm	4.5 keV/nm
Quartz	4.4 keV/nm	5.4 keV/nm

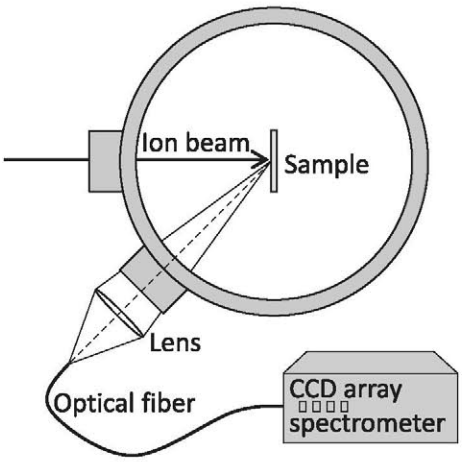

Fig. 1. Schematic representation of the experimental setup used to perform the ionoluminescence measurements.

of Fe^{3+} (band at 1.65 eV) [18,19], non-bridging oxygen hole centers (band at 1.9 eV) [9,10,20,21], radiative recombination of the self-trapped exciton with an E′ center (band at 2.26 eV) [18] and emission from self-trapped excitons (STE, band at 2.7 eV) [20–26]. It should be noted that some authors [27] have attributed the latter band to ODC-II (oxygen-deficient centers). However, one has to remark that in these cases the emission has been obtained in photoluminescence (PL) experiments after the irradiation. The response is different under direct ion irradiation (ionoluminescence), where the main involved process is the production of e–h pairs and eventually of self-trapped excitons (STE). Such processes have been reported in a number of experiments under irradiation (e.g., Messina et al. [21]), showing that the STE recombination yields the 2.7 eV emission (together with the NBOHC emission at 1.9 eV) and it also leads to the creation of intrinsic color centers. That assignment of the 2.7 eV IL emission has been also supported by theoretical calculations [23,26,28] and it appears, presently, a widely accepted idea. Anyhow, one cannot rule out some contribution of OCD-II emission (due to exciton recombination at these irradiation-induced centers), although this contribution is expected to be relatively small in comparison to the main recombination channel. The bands lying at 1.9 eV (652 nm) and 2.7 eV (459 nm) are far more intense than the others, as can be seen in Fig. 2. Consequently, we will focus the further discussion on them and hereafter they will be simply called the red and blue band, respectively.

For silica, one sees from Fig. 2 that the blue band is clearly dominant over the red one for low as well as for high fluences. For quartz, on the other hand, the red band dominates at low fluences but the blue one becomes more intense at the higher fluences. It should be noted that, in spite of the different IL spectra for the two materials at the initial stage of irradiation (Fig. 2a and b), they become nearly identical at the end of our irradiation process (Fig. 2c and d). Therefore, a detailed kinetic study is required to go deeper into the comparison.

The evolution of the IL yields for the two main bands (red and blue) as a function of fluence is shown in Fig. 3a and b for silica and quartz, respectively. Initially all curves exhibit a quasi-linear growth but then the behavior becomes more complicated and clearly different for the two SiO_2 phases. For *silica* both IL bands follow a rather similar kinetics but the blue band is clearly predominant over the red one for all irradiation cases and fluences, keeping a roughly constant ratio of about 5. The IL yields of both bands grow up to a maximum, reached below a fluence of around 10^{13} cm^{-2}, and then they strongly decrease down to a roughly steady value. For *quartz* the red band experiences a similar behavior as

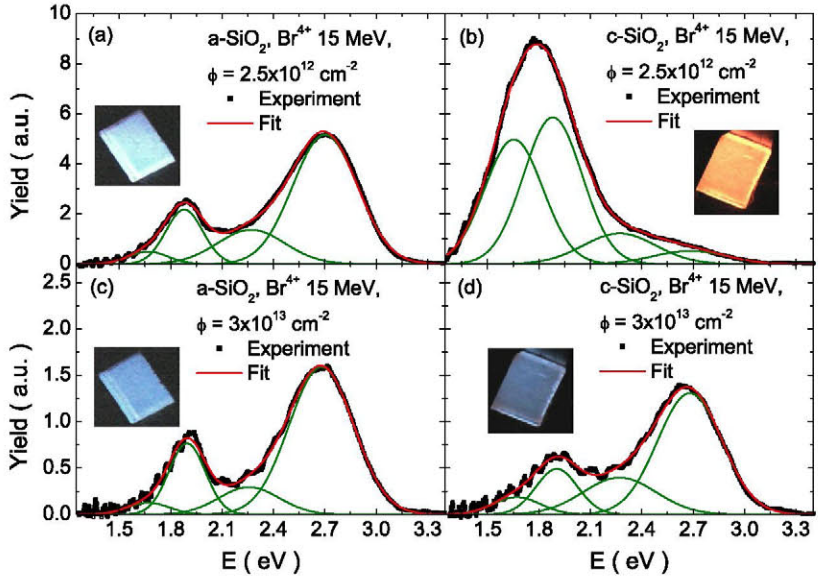

Fig. 2. Ionoluminescence spectra of silica irradiated with Br at 15 MeV for low (a) and high (c) fluences and for quartz irradiated with Br at 15 MeV for low (b) and high (d) fluences. The green curves represent the emission bands used to decompose the spectra.

Table 2
Peak positions, width and possible origin of the four emission bands obtained from the decomposition of the IL spectra.

Peak No.	Position (eV)	FWHM (eV)	Origin
1	1.65	0.30	$Fe^{3+} - >Si^{3+}$ [18,19]
2	1.9	0.35	NBOHC [10,18]
3	2.26	0.40	STE + E′ [18]
4	2.7	0.45	STE [22,23]

for silica, showing a maximum yield value at fluences $\approx 10^{13}$ cm^{-2}, followed by a fast monotonic decrease. The maximum yield is clearly higher than that observed for silica. On the other hand, the blue band initially presents a much smaller intensity and experiences a monotonic growth with fluence up to a saturation or slow-growth stage that appears close to but slightly lower than the final value reached in silica. This behavior suggests that after a high enough fluence we reach in both materials an equivalent "damaged" phase. One may also note that the maximum in the red band coincides with a slight change in the slope of the blue curve.

The ratio between the intensity of the blue and red peaks is also plotted in Fig. 4, for a better comparison. This ratio has the additional advantage of being independent of the experimental setup, which facilitates comparison with other experimental results. As can be seen, the growth of the blue peak with respect to the red one strongly depends on both, the material and the stopping power, being larger for silica and for the ion with the higher stopping power (Br at 15 MeV). In the saturation phase the Y_B/Y_R ratio reaches values independent of the incident ion and close to 2.4 and 3 for silica and quartz, respectively.

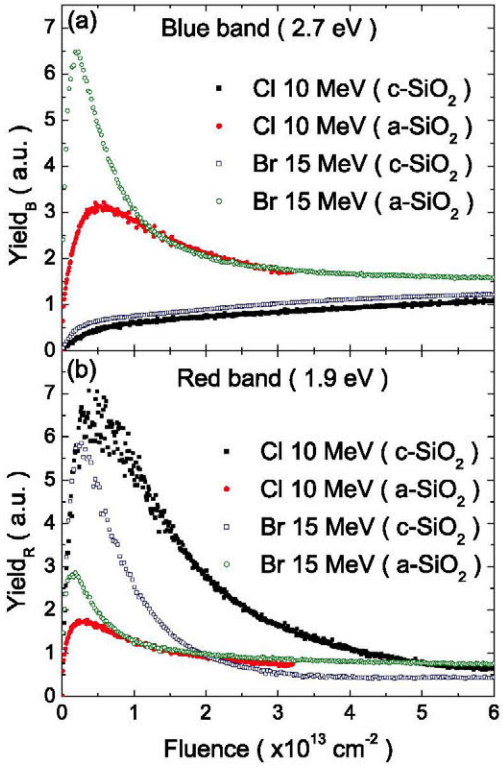

Fig. 3. Intensity of the blue (a) and red (b) bands as a function of the irradiation fluence for the ions and materials used in this work. (For interpretation of the references to colour in this figure legend, the reader is referred to the web version of this article.)

4. Discussion

In accordance with available results, our experimental data confirm that the same bands with similar optical parameters (peak energy and half-width) are observed in the IL spectra of both, the crystalline and amorphous SiO_2. The two main bands appear at 1.9 eV (red band) and 2.7 eV (blue band). As we discussed above, most authors attribute the red band to non-bridging oxygen hole centers (NBOHC) [10,20,21], having an unpaired electron in the 2p orbital along the broken Si–O bond. Moreover, the specific mechanism for the emission of the blue band is not yet definitely established although it appears to be related to emission from self-trapped excitons [22–26], preferentially located at strained bonds [26]. Recently, Ismail-Beigi and Louie [23] have confirmed, using an *ab initio* study, the role of straining on the self-trapping

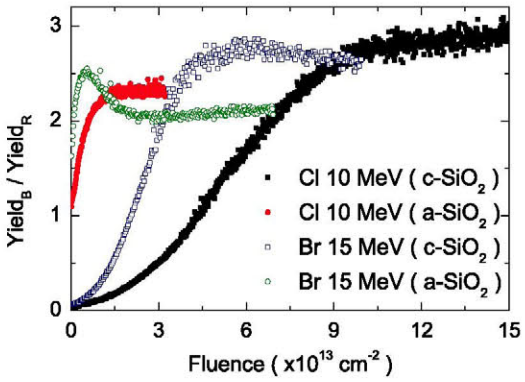

Fig. 4. Ratio between the yield intensity of the blue and red peaks (Y_B/Y_R) for the two materials and ions used in this work.

of excitons. They conclude that the formation of STE implies that the bond is broken, with the hole localized on the defected oxygen and the electron on the defected silicon atom in a planar sp^2 conformation. In line with this scenario we can now discuss our IL results.

For *silica*, the large number of strained bonds, due to structural reasons, accounts for the intense blue band that is predominant for all ions and fluences. Its height is about three times larger than that one for the red band. Moreover, this ratio keeps roughly constant throughout most of the irradiation suggesting some connection between the corresponding emission mechanisms. This behavior may be related to the results reported by Messina, Vaccaro and Cannas [21], using synchrotron radiation above the gap-energy threshold for SiO_2. They have ascertained that the 1.9 eV emission band accompanies the 2.7 eV emission band during STE decay. This has been interpreted as the NBOH centers being created at their excited states during the breaking of Si–O bond associated to the formation of the self-trapped excitons.

The overall kinetic behavior of the two bands in silica also deserves some comments. Both bands grow up to a maximum yield at a rather low similar fluence (2×10^{12} cm^{-2}) and then strongly decrease down to smaller values whose ratio is roughly $Y_B/Y_R \approx 3$. This reduction in the yield with increasing fluence is a relevant novel result of our experiments. The reason for this behavior is not clear and indeed it is not expected, given the constancy of the NBOHC concentration with fluence (after reaching the saturation stage) and the saturation or slow growth for the amorphization volume of the irradiated material [29]. This behavior could be related to the compaction effect induced by irradiation in silica. This irradiation-induced densification has been recently reported [29] and occurs for fluences similar to those at which the strong reduction in IL yield is produced. Some authors consider that this effect appears in parallel with the overlapping of individual ion tracks at high enough fluences [29]. The compaction effect reduces the bond strains leading to a more perfect structure (metamict phase [30,31]) closer to that of damaged quartz (see below). Then, this reduces the trapping capability for excitons [23,26].

For *quartz* the main result is the initial dominance of the red emission that progressively changes to the blue emission. This behavior is also consistent with the available information supporting that exciton self-trapping and recombination occurs preferentially at heavily strained Si–O bonds, such as those present in silica or in a damaged quartz crystal. In this respect, there is some experimental evidence that STE luminescence can be excited in a pristine quartz crystal using an electron pulse [32] or the second harmonic of an ArF laser [33]; however, it has been shown, using theoretical calculations [23,26,28], that the self-trapping is much more probable in the strained bonds. Another relevant feature from the experiments in quartz is that the IL kinetics for the blue band is quite different (even opposite) to that observed for silica. It experiences a monotonic rise up to a saturation or slow-growth stage without any sign of decrease. The behavior is quite comparable to that reported for the amorphization kinetics [34], as expected from the STE model discussed above. On the other hand, the red band presents a similar behavior to that observed for silica, i.e., growing up to a maximum followed by a marked decrease. In other words, for quartz there is no clear correlation between the evolution of the red and blue bands. Here, and pending a more quantitative analysis, one may invoke a competition between the recombination, either NBOHC or STE, sites. At the start of the irradiation few strained bonds are available for STE recombination. Therefore, most recombinations take place at NBOHC centers, already existing or produced by another mechanism. On increasing the extension of the irradiation-induced structural damage, the STE recombination channel grows and raises the contribution of the blue emission. Additional data are needed for a more complete understanding.

The above analysis is more clearly visualized by looking at Fig. 4. We observe that the relative growth of the blue band is much faster in silica than in quartz; probably this effect comes from the large number of stressed bonds preexisting on the former material while for the latter it is necessary to accumulate some damage before enough stressed bonds are produced and the blue peak appears. Moreover, the damaged stationary state is also reached much later in quartz than in silica. This effect can be explained if we consider that the crystalline structure represents a lower energy state (i.e., it is more stable) than the glassy structure while the damaged material represents an intermediate state between them. Thus, in terms of free energy it is much more convenient to pass from the vitreous phase than from the crystalline one to the damaged state; that's why the former transition occurs much earlier than the latter. Finally, the transitions occur before for higher stopping powers simply because more energy is being deposited on the lattice.

5. Conclusions

We have performed a detailed comparative experimental study of the IL induced by swift heavy ions on the two phases of high-purity SiO_2, either crystalline (quartz) or amorphous (silica). The results support the assignment of the blue emission band at 2.7 eV to recombination of self-trapped excitons at strained bonds that are initially present in silica and develop during irradiation in quartz. In silica, the data appear consistent with the assignment of the 1.9 eV emission band to NBOHC centers generated during the recombination of STE. The measured kinetic behavior, showing a strong reduction of the yield for the two emissions in silica, could be attributed to the compaction of the Si–O–Si network. For quartz, on the other hand, the kinetic behavior points out to a competition between recombination at NBOHC centers and STE sites. Although the presented results are mostly qualitative they offer relevant clues for a more quantitative and rigorous analysis that is currently underway.

Acknowledgments

This work has been supported by Spanish Ministry MICINN through the project MAT-2008-06794-C03-03, JCI-2009-05681, and by Madrid Community through the project TECHNOFUSION (S2009/ENE-1679). OPR is grateful to CONACyT, Mexico, for extending a postdoctoral fellowship.

References

[1] A. Moroño, E.R. Hodgson, Radiation induced optical absorption and radioluminescence in electron irradiated SiO_2, J. Nucl. Mater. 258–263 (1998) 1889–1892.

[2] J.F. Latkowski, A. Kubota, M.J. Caturla, S.N. Dixit, J.A. Speth, S.A. Payne, Fused silica final optics for inertial fusion energy: radiation studies and system-level analysis, Fusion Sci. Technol. 43 (2003) 540–558.

[3] N. Itoh, D.M. Duffy, S. Khakshouri, A.M. Stoneham, Making tracks: electronic excitation roles in forming swift heavy ion tracks, J. Phys.: Condens. Matter 21 (2009) 474205.

[4] Z.G. Wang, C. Dufour, E. Paumier, M. Toulemonde, The S_e sensitivity of metals under swift-heavy-ion irradiation: a transient thermal process, J. Phys.: Condens. Matter 6 (1994) 6733–6750.

[5] A. Kamarou, W. Wesch, E. Wendler, A. Undisz, M. Rettenmayr, Swift heavy ion irradiation of InP: thermal spike modeling of track formation, Phys. Rev. B. 73 (2006) 184107.

[6] N. Itoh, M. Stoneham, Materials modification by electronic excitation, Cambridge University Press, 2000.

[7] A. Rivera, A. Méndez, G. García, J. Olivares, J.M. Cabrera, F. Agulló-López, Ion-beam damage and non-radiative exciton decay in $LiNbO_3$, J. Lumin. 128 (2008) 703–707.

[8] F. Agulló-López, C.R.A. Catlow, P.D. Townsend, Point defects in materials, Academic Press, San Diego, CA, USA, 1988.

[9] S. Nagata, S. Yamamoto, K. Toh, B. Tsuchiya, N. Ohtsu, T. Shikama, et al., Luminescence in SiO_2 induced by MeV energy proton irradiation, J. Nucl. Mater. 329–333 (2004) 1507–1510.

[10] S. Nagata, S. Yamamoto, A. Inouye, B. Tsuchiya, K. Toh, T. Shikama, Luminescence characteristics and defect formation in silica glasses under H and He ion irradiation, J. Nucl. Mater. 367–370 (2007) 1009–1013.

[11] S.I. Kononenko, O.V. Kalantaryan, V.I. Muratov, V.P. Zhurenko, Silica luminescence induced by fast light ions, Radiat. Meas. 42 (2007) 751–754.

[12] P.D. Townsend, P.J. Chandler, L. Zhang, Optical effects of ion implantation, Cambridge University Press, Cambridge, UK, 1994.

[13] A.A. Bettiol, K.W. Nugent, D.N. Jamieson, The characterisation of high-grade synthetic quartz, corundum and spinel using ionoluminescence (IL), Nucl. Instrum. Meth. B. 130 (1997) 734–739.

[14] K.J. McCarthy, J.G. López, D.J. Rey, B. Zurro, A. Ibarra, A. Baciero, et al., The response of several luminescent materials to keV and MeV ions, J. Nucl. Mater. 340 (2005) 291–298.

[15] G. García, A. Rivera, M.L. Crespillo, N. Gordillo, J. Olivares, F. Agulló-López, Amorphization kinetics under swift heavy ion irradiation: a cumulative overlapping-track approach, Nucl. Instrum. Meth. B. 269 (2011) 492–497.

[16] CMAM – Centre for Micro Analysis of Materials, <http://www.cmam.uam.es/>. (2011).

[17] A.A. Finch, J. Garcia-Guinea, D.E. Hole, P.D. Townsend, J.M. Hanchar, Ionoluminescence of zircon: rare earth emissions and radiation damage, J. Phys. D Appl. Phys. 37 (2004) 2795–2803.

[18] M.A. Stevens-Kalceff, Cathodoluminescence microcharacterization of point defects in alpha-quartz, Mineral. Mag. 73 (2009) 585–605.

[19] G.E. King, A.A. Finch, R.A.J. Robinson, D.E. Hole, The problem of dating quartz 1: spectroscopic ionoluminescence of dose dependence, Radiat. Meas. 46 (2011) 1–9.

[20] L. Skuja, M. Hirano, H. Hosono, K. Kajihara, Defects in oxide glasses, Phys. Stat. Sol. C. 2 (2005) 15–24.

[21] F. Messina, L. Vaccaro, M. Cannas, Generation and excitation of point defects in silica by synchrotron radiation above the absorption edge, Phys. Rev. B. 81 (2010) 035212.

[22] N. Itoh, T. Shimizu-Iwayama, T. Fujita, Excitons in crystalline and amorphous SiO_2: formation, relaxation and conversion to Frenkel pairs, J. Non-Cryst. Sol. 179 (1994) 194–201.

[23] S. Ismail-Beigi, S.G. Louie, Self-trapped excitons in silicon dioxide: mechanism and properties, Phys. Rev. Lett. 95 (2005) 156401.

[24] A.N. Trukhin, Excitons in SiO_2: a review, J. Non-Cryst. Sol. 149 (1992) 32–45.

[25] S. Klaumünzer, Ion tracks in quartz and vitreous silica, Nucl. Instrum. Meth. B. 225 (2004) 136–153.

[26] R.M. Van Ginhoven, H. Jónsson, L.R. Corrales, Characterization of exciton self-trapping in amorphous silica, J. Non-Cryst. Sol. 352 (2006) 2589–2595.

[27] M. León, P. Martín, R. Vila, J. Molla, A. Ibarra, Vacuum ultraviolet excitation of the 2.7 eV emission band in neutron irradiated silica, J. Non-Cryst. Sol. 355 (2009) 1034–1037.

[28] R.M. Van Ginhoven, H. Jónsson, K.A. Peterson, M. Dupuis, L.R. Corrales, An ab initio study of self-trapped excitons in α-quartz, J. Chem. Phys. 118 (2003) 6582–6593.

[29] J. Manzano, J. Olivares, F. Agulló-López, M.L. Crespillo, A. Moroño, E. Hodgson, Optical waveguides obtained by swift-ion irradiation on silica (a-SiO_2), Nucl. Instrum. Meth. B. 268 (2010) 3147–3150.

[30] A. Vanelstraete, C. Laermans, Tunneling states in neutron-irradiated quartz: measurements of the ultrasonic attenuation and velocity change, Phys. Rev. B. 42 (1990) 5842–5854.

[31] V. Keppens, C. Laermans, Direction dependence of the tunneling states-phonon coupling in neutron irradiated quartz, Physica B 263–264 (1999) 149–151.

[32] C. Itoh, K. Tanimura, N. Itoh, Optical studies of self-trapped excitons in SiO_2, J. Phys. C 21 (1988) 4693–4702.

[33] A.N. Trukhin, Self-trapped exciton singlet-triplet splitting in crystals with α-quartz structure: SiO_2, SiO_2–Ge, GeO_2, $AlPO_4$ and $GaPO_4$, J. Phys.: Condens. Matter 20 (2008) 125217.

[34] J. Manzano-Santamaría, J. Olivares, A. Rivera, F. Agulló-López, Electronic damage in quartz (c-SiO_2) by MeV ion irradiations: potentiality for optical waveguiding applications, Nucl. Instrum. Meth. B 272 (2012) 271–274.

[35] J. Ziegler, SRIM – The Stopping and Range of Ions in Matter: http://www.srim.org/, (2008).

[36] J.F. Ziegler, The stopping and range of ions in solids, Pergamon Press, 1985.